Suppression of Innate Immune Pathology by Regulatory T Cells during Influenza A Virus Infection of Immunodeficient Mice[∇][†]

Inês Antunes and George Kassiotis*

Division of Immunoregulation, MRC National Institute for Medical Research, The Ridgeway, London NW7 1AA, United Kingdom

The viral infection of higher vertebrates elicits potent innate and adaptive host immunity. However, an excessive or inappropriate immune response also may lead to host pathology that often is more severe than the direct effects of viral replication. Therefore, several mechanisms exist that regulate the magnitude and class of the immune response. Here, we have examined the potential involvement of regulatory T (Treg) cells in limiting pathology induced by influenza A virus (IAV) infection. Using lymphocyte-deficient mice as hosts, we showed that Treg cell reconstitution resulted in a significant delay in weight loss and prolonged survival following infection. The adoptively transferred Treg cells did not affect the high rate of IAV replication in the lungs of lymphocyte-deficient hosts, and therefore their disease-ameliorating effect was mediated through the suppression of innate immune pathology. Mechanistically, Treg cells reduced the accumulation and altered the distribution of monocytes/macrophages in the lungs of IAV-infected hosts. This reduction in lung monocytosis was associated with a specific delay in monocyte chemotactic protein-2 (MCP-2) induction in the infected lungs. Nevertheless, Treg cells failed to prevent the eventual development of severe disease in lymphocyte-deficient hosts, which likely was caused by the ongoing IAV replication. Indeed, using T-cell-deficient mice, which mounted a T-cell-independent B cell response to IAV, we further showed that the combination of virus-neutralizing antibodies and transferred Treg cells led to the complete prevention of clinical disease following IAV infection. Taken together, these results suggested that innate immune pathology and virus-induced pathology are the two main contributors to pathogenesis during IAV infection.

Viruses are obligate intracellular parasites that infect host cells to complete their life cycle. Viruses may differ substantially in the amount of host cell damage they cause during their replication (7, 17, 57, 62, 67). The immune response presents a powerful barrier against viruses and can target both cell-free viruses and virus-infected cells. However, left uncontrolled, the immune response may cause more damage to host cells, infected or uninfected, than the replication of the virus would (20, 24).

Regulatory T (Treg) cells are a subset of CD4^{+} T cells with naturally endowed immune-suppressive activity (51, 52). It is becoming increasingly clear that Treg cells can affect the immune response not only to self antigens but also to infecting viruses (6, 48, 51, 52). An involvement of Treg cells in shaping the immune response to and protection against viruses has been observed in almost every type of infection that has been studied (6, 48). However, the activities of Treg cells to hinder or help the host in its effort to eliminate the infecting virus can be as divergent as the viruses themselves. For example, Treg cells have been shown to suppress the induction or effector function of the adaptive immune response to Friend virus (FV) (12, 21), West Nile virus (30), herpes simplex virus type 1 (HSV-1) (53), or respiratory syncytial virus (RSV) (50), which was consistently associated with reduced virus control (30, 50,

53, 70). However, the suppression of adaptive immunity by Treg cells led to worse clinical outcomes in infection with WNV (30) or RSV (50), whereas it was accompanied with the reduction of immune pathology and better clinical outcome in infection with FV (3) or HSV-1 (53). Perhaps less expected was the observation that the lack of Treg cell-mediated suppression compromised the ability of the host to coordinate the earliest stages of the immune response in genital mucosa following local infection with HSV-2 or in the liver following systemic infection with lymphocytic choriomeningitis virus (LCMV) (35). Thus, the overall effect of Treg cells on immunity to and pathology from viral infection is influenced by the nature of the infection.

The mediators and cellular targets of Treg cell suppression are similarly diverse (33, 51, 56, 65). Treg cells secrete or display on their membrane an array of immune-suppressive molecules that can act directly on target cells (56, 65). Treg cells also can mediate suppression indirectly by competition for growth factors or homeostatic space (56, 59, 65). To exert the suppression of diverse target cell types and in different inflammatory contexts, Treg cells may rely on one particular mechanism for suppression, or they may display some degree of flexibility and redundancy in the mediators they use (56, 65). For example, the conditional ablation of interleukin-10 (IL-10) in Treg cells has resulted in spontaneous colitis in mice housed in specific-pathogen-free facilities and enhanced immune reactivity in the lungs of mice additionally sensitized with ovalbumin inhalation (49). However, the loss of Treg cell-produced IL-10 did not lead to systemic autoimmunity (49). In contrast, the conditional ablation of CTLA-4 in Treg cells has been reported to cause systemic inflammatory manifestations (68). Recently, the newly identified cytokine IL-35 has been estab-

* Corresponding author. Mailing address: Division of Immunoregulation, MRC National Institute for Medical Research, The Ridgeway, Mill Hill, London NW7 1AA, United Kingdom. Phone: 44 (0) 2088 162 354. Fax: 44 (0) 2088 162 564. E-mail: gkassio@nimr.mrc.ac.uk.
† Supplemental material for this article may be found at http://jvi.asm.org/.
∇ Published ahead of print on 13 October 2010.

lished by one study as an important contributor to the suppressive activity of Treg cells, especially when directed against effector T cells (9). In addition to effector T cells, B cells, dendritic cells, macrophages, and natural killer cells are included in the expanding range of cellular targets of Treg cells (56). For instance, Treg cells have been shown to suppress innate immune-driven inflammation and intestinal pathology in lymphocyte-deficient mice infected with the bacterial pathogen *Helicobacter hepaticus* (37). It is therefore clear that Treg cells have the potential to regulate the pathology arising from the innate immune response to infection.

One viral infection, the pathogenesis of which is thought to involve dysregulated immune reaction, is infection with influenza A virus (IAV) (36, 44, 62). IAV is a highly cytopathic virus that causes infected epithelial cell necrosis and extensive damage to the respiratory system (36, 62). Several studies of human and animal models have suggested that the severity of highly pathogenic IAV infection correlates with an exuberant immune reaction with the massive accumulation of macrophages into the lungs and the overabundance of inflammatory cytokines and chemokines in the lungs and serum (5, 8, 10, 25, 28, 36, 44, 45, 62, 63). However, the relative contribution of direct cytopathic effects of viral replication or of an excessive or inappropriate immune reaction to the pathogenesis of IAV infection remains unclear (36, 44, 62). The pathogenic contribution of the T-cell response to IAV has been highlighted in studies using the mouse as a host (26, 31, 40). However, the rapidity with which IAVs, especially newly emerged highly pathogenic strains, induce pathology suggests that innate immunity is a main contributor (36, 44, 62).

Here, we examined the course of IAV infection in lymphocyte-deficient $Rag1^{-/-}$ mice, where any contribution of adaptive immunity to either infection-induced pathology or antiviral immunity can be excluded. We have concentrated on a potential suppressive effect of Treg cells on any host response to IAV other than the adaptive response, collectively referred to as the innate immune response. The rationale behind this approach was that the potential benefit provided by immune-suppressive Treg cells would correspond to the minimum contribution of innate immunity to IAV-induced pathology, whereas direct cytopathic effects of the virus would not be affected. Thus, the presence of Treg cells during the IAV infection of $Rag1^{-/-}$ mice could discriminate between immune- and virus-mediated pathogenic effects.

MATERIALS AND METHODS

Mice. Inbred C57BL/6 (B6), BALB/c (C), and BALB/c-nude (C-$Foxn1^{nu}$) mice originally were obtained from the Jackson Laboratory (Bar Harbor, ME) and subsequently were maintained at National Institute for Medical Research (NIMR) animal facilities. B6-backcrossed Rag1-deficient mice (B6.129S7-$Rag1^{tm1Mom}$/J or $Rag1^{-/-}$) have been described previously (39) and also were maintained at NIMR animal facilities. All animal experiments were approved by the ethical committee of the NIMR and conducted according to local guidelines and United Kingdom Home Office regulations.

Influenza A infection. Nonanesthetized mice were infected with 250 hemagglutinin units (HAU) of the A/PR/8/34 (PR8) (H1N1) strain of IAV by instillation into their nasal cavities. For intravenous influenza infection, mice received an inoculum of 250 HAU of PR8, injected via the tail vein in 0.1 ml of phosphate-buffered saline. Body weight was monitored daily after infection, and mice were culled when their weight dropped bellow 75% of the average weight of a strain-, age-, and gender-matched control group.

Virus-neutralizing antibody response. Serum titers of IAV-neutralizing antibodies were measured as previously described (26). Briefly, sera were collected on days 6 and 12 after PR8 infection, heat inactivated for 10 min at 56°C, and tested using a modified Madin-Darby canine kidney (MDCK)-based assay. Serial dilutions of the sera were added to monolayers of MDCK cells in 96-well plates, which subsequently were infected with a 95% tissue culture-infective dose of PR8. MDCK cell viability was measured with an Alamar blue-based assay 3 days after infection. Cultures were pulsed with Alamar blue for 1 to 2 h, and fluorescence was measured with a fluorescence plate reader (PerkinElmer LS50B).

T-cell purification and adoptive transfer. $CD25^-$ $CD4^+$ or $CD25^+$ $CD4^+$ T cells were isolated from the spleens and lymph nodes of donor mice using immunomagnetic positive selection (EasySep beads; StemCell Technologies, Vancouver, British Columbia, Canada) according to the manufacturer's instructions. Enriched cell suspensions were stained with antibodies to surface markers and then further purified by cell sorting, which was performed on MoFlo cell sorters (Dako, Fort Collins, CO). Typical cell purity following cell sorting was higher than 98%. Purified cells (1×10^6 per recipient) were injected in recipient mice via the tail vein in 0.1 ml of air-buffered Iscove's modified Dulbecco's medium (IMDM).

Flow-cytometric analysis. Single-cell suspensions were prepared from the spleens or the lungs of donor mice, and mononuclear cells from the lungs were further enriched using Histopaque 1083 (Sigma-Aldrich, St. Louis, MO) by following the manufacturer's instructions. Cells subsequently were stained with directly conjugated antibodies to surface markers, which were obtained from eBiosciences (San Diego, CA), CALTAG/Invitrogen (Carlsbad, CA), or BD Biosciences (San Jose, CA). FoxP3 was detected by intranuclear staining using a FoxP3 staining kit (eBiosciences) according to the manufacturer's instructions. Cytometry was performed on a FACSCalibur (BD Biosciences) flow cytometer and analyzed with FlowJo v8.7 (Tree Star Inc., Ashland, OR) analysis software.

Analysis of serum cytokine and chemokine levels. Serum was prepared from blood samples, which were allowed to clot at 4°C. Serum cytokine levels were analyzed by a Bio-plex cytokine assay (Bio-Rad Laboratories, Ltd., United Kingdom) on a Luminex 100 instrument (Bio-Rad Laboratories, Ltd., United Kingdom). MCP-2 levels were analyzed using a mouse CCL8/MCP-2 enzyme-linked immunosorbent assay (ELISA) kit (IBL International GmbH, Hamburg, Germany).

RNA purification and cDNA preparation. Total RNA was extracted from whole tissues using TRI reagent (Sigma-Aldrich) and subsequently was used for cDNA synthesis with the Omniscript reverse transcription (RT) kit (Qiagen, Hilden, Germany). Briefly, 1 ng of RNA was used as the template, and cDNA synthesis was primed by a mixture of 1 μM random hexamers and 1 μM of a primer specific to a highly conserved region of the IAV *matrix* gene (5'-TCTA ACCGAGGTCGAAACGTA-3'), as previously described (66). Reaction mixtures were incubated at 37°C for 1 h and terminated by incubating the mixture at 90°C for 5 min.

qRT-PCR. Expression of mRNA was determined by quantitative RT-PCR (qRT-PCR) using a DNA master SYBR green I kit (Roche, Mannheim, Germany) and the ABI Prism 7000 detection system (TaqMan, Applied Biosystems, Foster City, CA). The following primers were used for the amplification of target transcripts: *Hprt* forward (5'-TTGTATACCTAATCATTATGCCGAG-3') and reverse (5'-CATCTCGAGCAAGTCTTTCA-3'), IAV *matrix* (66) forward (5'-AAGACCAATCCTGTCACCTCTGA-3') and reverse (5'-CAAAGCGTCTAC GCTGCAGTCC-3'), and *Ccl8* forward (5'-CTGGAGAGCTACACAAGAA-3') and reverse (5'-TCTGACTCTCAGTCCATGT-3'). Samples were analyzed in duplicate. The housekeeping gene *Hprt* was used to normalize the critical threshold values for the genes of interest. Levels of IAV *matrix* mRNA are plotted as arbitrary units relative to *Hprt* mRNA levels. Levels of *Ccl8* mRNA are plotted as the fold induction compared to those in naïve uninfected $Rag1^{-/-}$ mice, which were given a value of 1.

Microarray analysis. Microarray analysis was performed with RNA isolated from total lungs. Three biological replicates were used for each of the following groups: uninfected $Rag1^{-/-}$ control mice (group 1) and PR8-infected $Rag1^{-/-}$ mice in the presence (group 2) or absence (group 3) of adoptively transferred Treg cells, measured on day 15 postinfection. Probe labeling and hybridization were performed using MouseGene 1.0 ST oligonucleotide arrays (Affymetrix, Santa Clara, CA). Primary microarray data were analyzed with GeneSpring GX (Agilent Technologies, Inc., Santa Clara, CA).

Histology and immunohistochemistry. For histological examination, lungs were dissected from donor mice and immersion fixed for 24 h in 5% buffered formaldehyde solution, dehydrated in a series of graded alcohols, and embedded in paraffin. Sections were cut from five levels of the paraffin blocks and stained with hematoxylin and eosin. Histological sections were examined and photographed under light microscopy. For immunohistochemistry, lungs were embed-
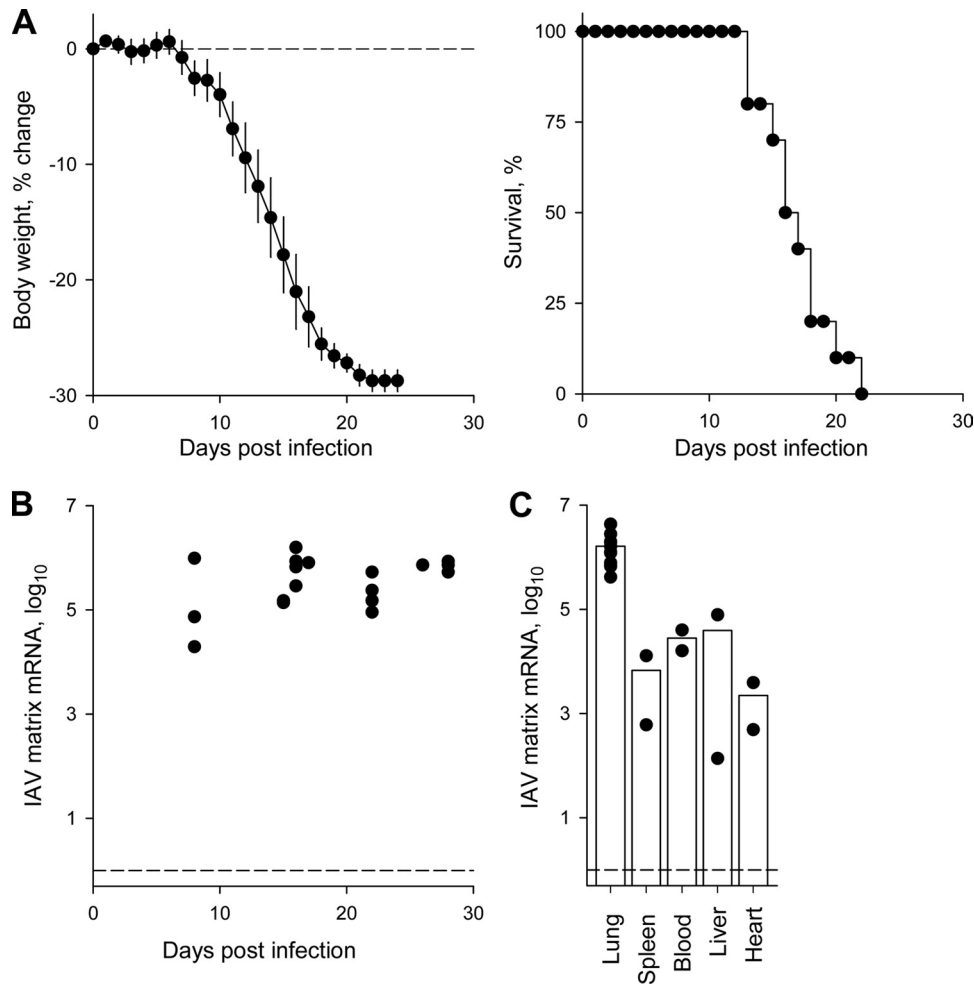
FIG. 1. Protracted IAV infection in lymphocyte-deficient mice. (A) Weight change (left) and survival (right) of $Rag1^{-/-}$ mice following intranasal infection with PR8. Infected mice were monitored daily and culled when they reached an endpoint of 25% weight loss. Data are compiled from >15 mice analyzed in three separate experiments. Median survival time after PR8 infection was 17.8 days. (B) Levels of PR8 *matrix* mRNA in the lungs of PR8-infected $Rag1^{-/-}$ mice determined by qRT-PCR over time. Each symbol represents an individual mouse. (C) Levels of PR8 *matrix* mRNA in the indicated organs from infected $Rag1^{-/-}$ mice, measured 15 days following PR8 infection. Each symbol represents an individual mouse, and bars denote the mean level in each organ.

ded in OCT compound (Dako) and frozen. Frozen lung sections were fixed in cold acetone and subsequently were stained with an anti-mouse CCL8/MCP-2 monoclonal antibody (R&D Systems, Minneapolis, MN) followed by a secondary goat anti-rat antibody IgG conjugated to Alexa Fluor647 (Invitrogen). Sections also were counterstained for nuclei with Hoechst 33258 (Sigma-Aldrich). Stained sections were mounted in fluorescent mounting medium (Dako) and viewed with a Leica TCS SP2 AOBS confocal microscope. Images were acquired with Leica confocal software using the 20× or 40× objective lens.

Statistical analysis. Statistics were generated by Student's *t* test performed using SigmaPlot v10 software (Systat Software Inc., San Jose, CA).

RESULTS

Protracted IAV infection in lymphocyte-deficient mice. To facilitate the study of the innate response to IAV infection and the potential direct effect of Treg cells on innate immunity, we have used lymphocyte-deficient $Rag1^{-/-}$ mice as hosts, in which a confounding effect of adaptive immunity was absent. PR8-infected $Rag1^{-/-}$ mice started losing body weight, which was used as a measure of pathology, on average from day 7 of infection and reached an endpoint of 25% body weight loss, at

which point they were culled, in a median of 17.8 days (Fig. 1A). Viral replication in the lungs, assessed by qRT-PCR for *matrix* mRNA, was very high from the onset of symptoms and, as expected for lymphocyte-deficient hosts, remained high throughout the course of infection (Fig. 1B). In the absence of an adaptive immune response, IAV has the potential to spread beyond the lungs and thus cause mortality due to systemic manifestations. We therefore looked for the presence of viral mRNA in organs other than the lungs. Indeed, PR8 *matrix* mRNA was readily detected in the circulation and in all organs tested (Fig. 1C). However, the relative presence of PR8 *matrix* mRNA was at least one order of magnitude higher in the lungs than in any other anatomical location (Fig. 1C), indicating that IAV was replicating primarily in the lungs. In addition, we were unable to isolate infectious particles of PR8 from any location other than the lungs (data not shown), suggesting that the systemic presence of viral RNA was not associated with productive infection. As it was important to establish that the pathology developing during IAV infection of $Rag1^{-/-}$ mice
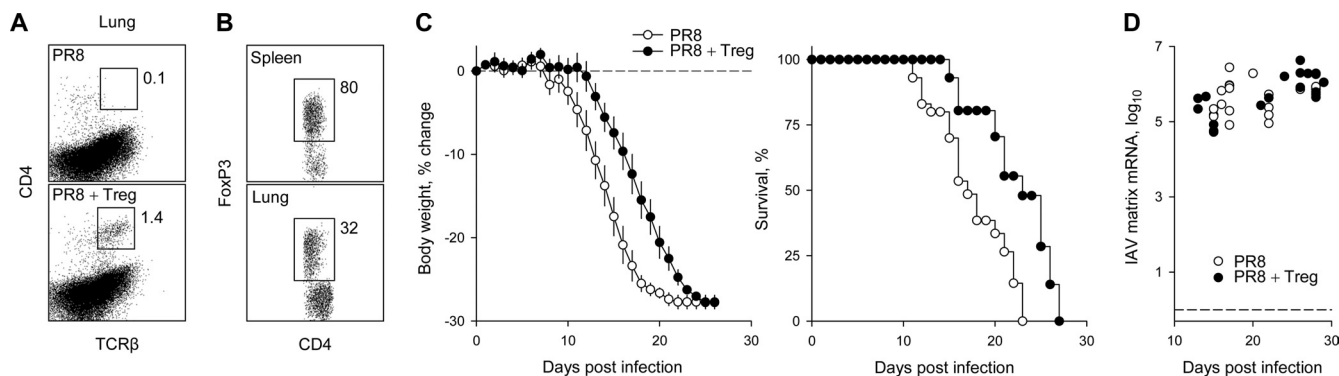
FIG. 2. Effect of Treg cell transfer on the course of IAV infection of lymphocyte-deficient mice. (A) Flow-cytometric detection of transferred Treg cells in the lungs of PR8-infected $Rag1^{-/-}$ mice (PR8 + Treg). As a control, the lungs of PR8-infected $Rag1^{-/-}$ mice that did not receive Treg cells (PR8) also were analyzed. Numbers within the plots represent the mean percentage of CD4$^+$ TCRβ$^+$ T cells in 5 to 9 mice per group analyzed 20 to 25 days after PR8 infection. (B) Percentage of Foxp3$^+$ cells in CD4$^+$ TCRβ$^+$ T cells isolated from the spleen or the lungs of PR8-infected $Rag1^{-/-}$ recipients of Treg cell transfer. Numbers within the plots represent the mean percentages of Foxp3$^+$ cells in six mice analyzed 25 days after PR8 infection. (C) Weight change (left) and survival (right) of PR8-infected $Rag1^{-/-}$ mice in the presence (PR8 + Treg) or absence (PR8) of adoptively transferred Treg cells. Data are from 12 mice analyzed in three separate experiments. Median survival times were 18.0 days for PR8 and 22.5 days for PR8 + Treg ($P = 0.004$). (D) Levels of PR8 *matrix* mRNA over time in the lungs of PR8-infected $Rag1^{-/-}$ mice with (PR8 + Treg) or without (PR8) adoptively transferred Treg cells. Each symbol represents an individual mouse.

was due to viral replication in the lungs, we compared intranasal infection, which would start in the lungs before spreading to other organs, to intravenous infection, which would follow the opposite route. Intranasally and intravenously infected $Rag1^{-/-}$ mice progressed to the weight loss endpoint at a comparable rate (see Fig. S1A in the supplemental material), and furthermore, levels of PR8 *matrix* mRNA in intravenously infected mice was higher in the lungs than in any other location (see Fig. S1B in the supplemental material). Taken together, these results indicated that PR8 replication following the infection of $Rag1^{-/-}$ mice was largely confined to the lungs.

Treg cells delay IAV-induced mortality in lymphocyte-deficient hosts. To study the effect of Treg cells on the innate immune response to IAV, we adoptively transferred fluorescent-activated cell sorter (FACS)-purified CD25$^+$ CD4$^+$ T cells from virus-naïve donor mice into PR8-infected $Rag1^{-/-}$ recipients. The transferred T cells were found in the lungs of infected mice (Fig. 2A), suggesting that they could be mediating a local effect. The majority (~80%) of transferred T cells recovered from the spleens of recipient mice were found to express FoxP3 until day 25 posttransfer, the last time point examined (Fig. 2B). However, the percentage of FoxP3$^+$ cells among donor-type CD4$^+$ T cells was lower in the lungs (~30%) than in the spleens of infected recipients (Fig. 2B). Nevertheless, FoxP3$^+$ cells were present at highly elevated frequencies even in the lungs of infected recipients compared to those for naïve wild-type mice. The transfer of Treg cells had a significant effect on disease development in IAV-infected $Rag1^{-/-}$ recipients, extending their survival by an average of 4.5 days (25%) compared to that of control PR8-infected $Rag1^{-/-}$ mice that did not receive Treg cells (Fig. 2C). The abundance of IAV *matrix* mRNA, an indicator of viral replication, was comparable between infected mice that received Treg cells and those that did not (Fig. 2D), suggesting that Treg cells delayed disease development by a mechanism other than direct virus control. To confirm that the prolonged survival of infected $Rag1^{-/-}$ recipients was mediated by Treg cells

in the inoculum rather than by FoxP3$^-$ potential effector T cells, we compared the survival of infected $Rag1^{-/-}$ mice to that of mice receiving an inoculum of Treg cell-depleted naïve CD25$^-$ CD44^{low} CD4$^+$ T cells, which would differentiate almost exclusively into effector T cells. The transfer of naïve CD4$^+$ T cells accelerated the weight loss of infected $Rag1^{-/-}$ recipients (see Fig. S2A in the supplemental material) and also caused a small decrease in viral mRNA levels in the lungs (see Fig. S2B in the supplemental material). These results indicated that the adoptive transfer of Treg cells extended the survival of PR8-infected $Rag1^{-/-}$ recipients, whereas the transfer of Treg cell-depleted naïve CD4$^+$ T cells had the opposite effect.

To examine the mechanisms by which Treg cells were exerting their pathology-reducing effect, we initially tested the requirement for the production of immune-suppressive cytokines. Treg cell production of IL-10 and, more recently, of the newly identified interleukin-35 (IL-35) have been implicated in the suppression of immune-mediated pathology in several systems (2, 9, 19, 23, 27, 44, 49). However, Treg cells isolated from either $Il10^{-/-}$ or $Il12a^{-/-}$ mice (unable to produce IL-35) were as efficient as wild-type Treg cells in prolonging the survival of PR8-infected $Rag1^{-/-}$ recipients (Fig. 3), indicating that neither of these two cytokines was critically required.

Treg cells reduce lung monocytosis in lymphocyte-deficient hosts. To further study the mechanisms by which Treg cell transfer was impinging on IAV infection-induced pathology in lymphocyte-deficient hosts, we performed a microarray analysis of lung transcriptome changes on day 15 after PR8 infection. Compared to levels for uninfected mice, the PR8 infection of $Rag1^{-/-}$ mice induced >2-fold changes in the expression of ~1,200 genes, with ~120 genes displaying >4-fold overrepresentation, heavily dominated by interferon-inducible and immune-related gene transcripts (see Table S1 in the supplemental material). Interestingly, some of the most highly induced gene transcripts (5- to 15-fold induction) represented genes specifically expressed in cells of the monocyte/macrophage lineage, such as complement component 3a re-
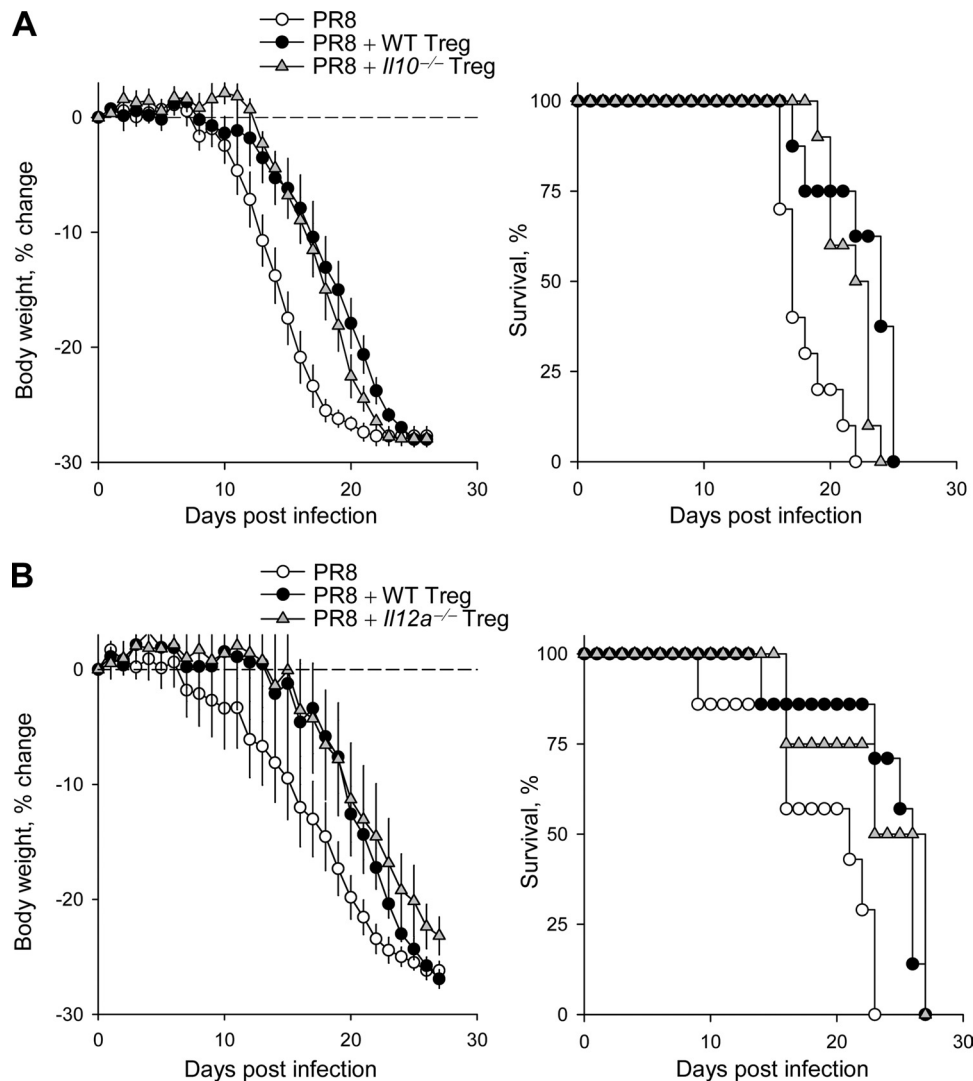
FIG. 3. Treg cells delay the symptoms of IAV infection of lymphocyte-deficient mice independently of IL-10 or IL-35. (A) Weight change (left) and survival (right) of PR8-infected $Rag1^{-/-}$ mice in the presence of wild-type (PR8 + WT Treg) or $Il10^{-/-}$ Treg cells (PR8 + $Il10^{-/-}$ Treg) or in the absence of Treg cells (PR8). Data are from 10 to 12 mice analyzed in two separate experiments. Median survival times were 17.8 days (PR8), 22.3 days (PR8 + WT Treg), and 21.7 days (PR8 + $Il10^{-/-}$ Treg). (B) Weight change (left) and survival (right) of PR8-infected $Rag1^{-/-}$ mice in the presence of wild-type (PR8 + WT Treg) or $Il12a^{-/-}$ Treg cells (PR8 + $Il12a^{-/-}$ Treg) or in the absence of Treg cells (PR8). Data are from 9 to 10 mice analyzed in two separate experiments. Median survival times were PR8 = 18.6 (PR8), 23.9 days (PR8 + WT Treg), and 23.3 days (PR8 + $Il10^{-/-}$ Treg).

ceptor 1 (*C3ar1*), myeloid cell nuclear differentiation antigen (*Mnda*), and the high-affinity Fc receptor for IgG (*Fcgr1*) (Fig. 4A), indicating monocytic overrepresentation in the IAV-infected lung. To confirm that the lungs of PR8-infected $Rag1^{-/-}$ mice were indeed characterized by monocytosis, as suggested by the microarray analysis, we analyzed the cellular composition of single-cell lung suspensions by flow cytometry (Fig. 4B). Compared to results from uninfected $Rag1^{-/-}$ mice, lungs, but not spleens, from $Rag1^{-/-}$ mice infected with PR8 15 days previously consisted predominantly of mononuclear cells with higher light scatter (Fig. 4B). These cells were most closely related to the monocyte/macrophage lineage, as they expressed high levels of CD11b and Gr1 (Ly-6C$^+$ but Ly-6G$^-$) and intermediate levels of CD11c, and they also were positive for

major histocompatibility complex class II (MHC-II) and F4/80 (Fig. 4C).

We next investigated the effect of Treg cell transfer on lung monocytosis in PR8-infected $Rag1^{-/-}$ mice throughout the course of infection. Monocyte/macrophage numbers rose steadily in the lungs of PR8-infected $Rag1^{-/-}$ mice from day 7 postinfection until the termination of the experiment compared to results for uninfected mice (Fig. 5A). The adoptive transfer of Treg cells significantly delayed the rate of monocyte/macrophage accumulation in the lungs ($P = 0.016$ for all time points combined) (Fig. 5A). This delay also was evident at late time points ($P = 0.006$ post day 20) (Fig. 5A), when disease severity in PR8-infected $Rag1^{-/-}$ recipients of Treg cells approached that of control mice. Thus, Treg cells
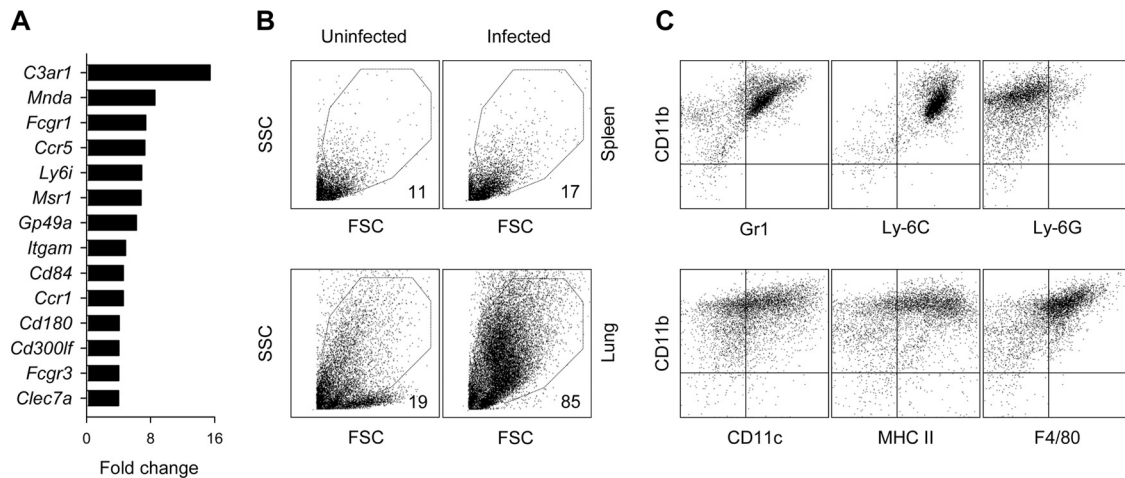
FIG. 4. Monocyte/macrophage accumulation in the lungs of IAV-infected lymphocyte-deficient mice. (A) Fold change in the transcription of monocyte/macrophage-specific genes, measured by microarray analysis 15 days following PR8 infection of $Rag1^{-/-}$ mice, compared to uninfected $Rag1^{-/-}$ control mice. (B) Forward (FSC) and side scatter (SSC) cytometric profile of mononuclear cells isolated from the spleens (top) or the lungs (bottom) of PR8-infected or uninfected $Rag1^{-/-}$ mice. Numbers within the plots represent the mean percentage of FSC^{high} SSC^{high} cells in five to seven mice per group per organ 15 to 20 days after PR8 infection. (C) Expression of myeloid cell markers by FSC^{high} SSC^{high} cells from the lungs of PR8-infected $Rag1^{-/-}$ mice 20 days postinfection.

significantly reduced lung monocytosis throughout the PR8 infection of $Rag1^{-/-}$ mice, even though these mice did eventually succumb to severe IAV-induced pathology. The histological examination of lung sections revealed that, compared to those from uninfected control mice, the lungs of PR8-infected $Rag1^{-/-}$ mice were noticeably more inflamed independently of the presence of Treg cells (Fig. 5B). However, this lung inflammation and mononuclear cell infiltration were more localized and confined to distinct areas in mice that had received Treg cells than in those that had not, where mononuclear cell infiltrates were distributed evenly throughout the tissue (Fig. 5B). Furthermore, cells with monocytic morphology were fre-

quently engulfing polymorphonuclear cells, likely neutrophils, only in Treg cell recipients (Fig. 5B). Thus, the transfer of Treg cells into PR8-infected $Rag1^{-/-}$ mice altered both the number and relative distribution of monocytes/macrophages in the inflamed lung, suggesting that Treg cells control the recruitment or migration of these inflammatory cells.

Selective suppression of *Ccl8* and *Cxcl13* induction by Treg cells. To further dissect the mechanisms by which Treg cells have been affecting the extent of lung monocytosis in PR8-infected $Rag1^{-/-}$ mice, we looked for changes in the transcriptional activity of chemokine genes. Compared to results for uninfected controls, transcripts for chemokine (C-C motif) li-
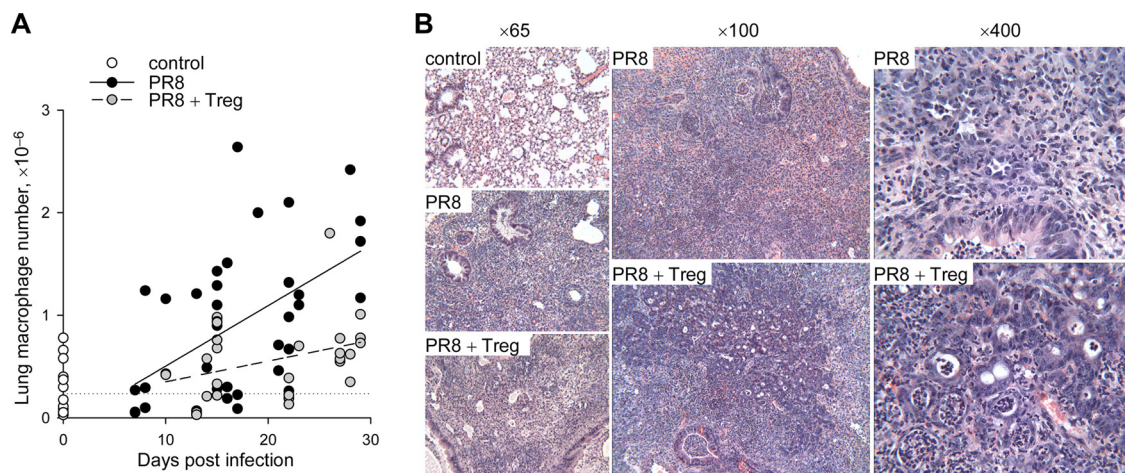

FIG. 5. Effect of Treg cell transfer on monocyte/macrophage accumulation in the lungs of IAV-infected lymphocyte-deficient mice. (A) Absolute numbers of monocytes/macrophages over time in the lungs of PR8-infected $Rag1^{-/-}$ mice in the presence (PR8 + Treg) or absence (PR8) of adoptively transferred Treg cells. For comparison, absolute numbers of monocytes/macrophages in the lungs of uninfected $Rag1^{-/-}$ control mice also are shown at time zero, and their averages are depicted by the dotted line. Each symbol represents an individual mouse. (B) Light microscopy photographs of hematoxylin/eosin-stained sections from the lungs of uninfected $Rag1^{-/-}$ control mice (control) or PR8-infected $Rag1^{-/-}$ mice in the presence (PR8 + Treg) or absence (PR8) of adoptively transferred Treg cells. Numbers at the top of each column denote the magnification. Sections are representative of 3 to 4 mice per group analyzed 15 days postinfection.
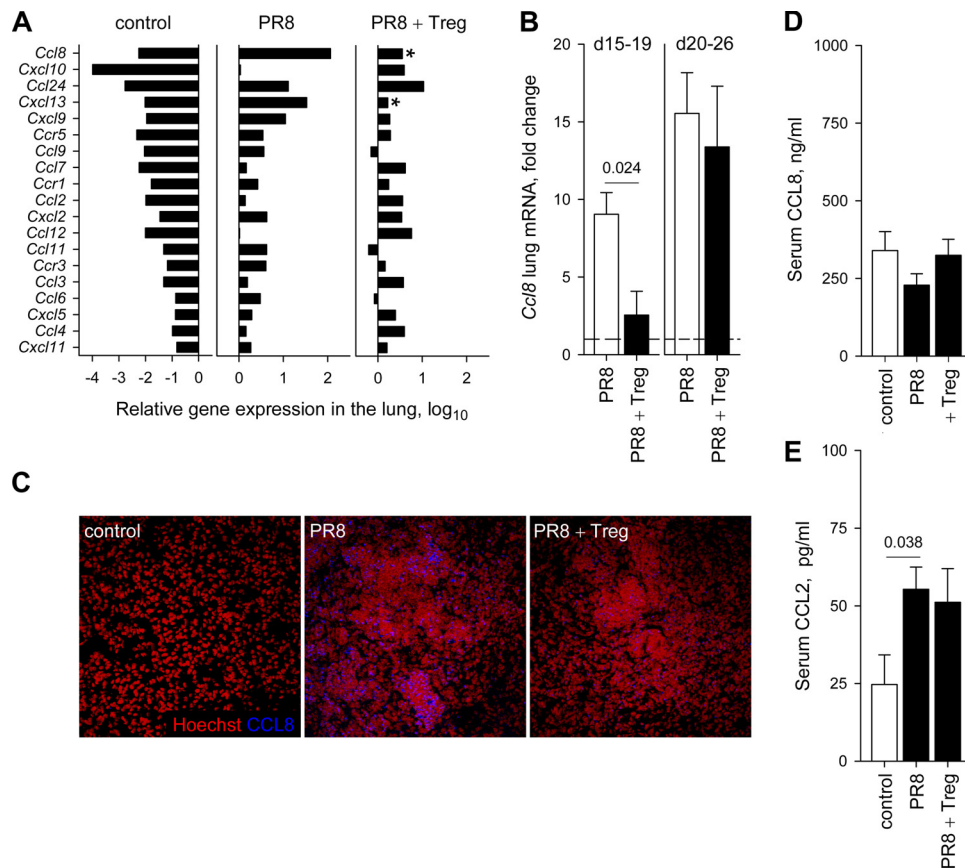
FIG. 6. Treg cells alter the pattern of chemokine expression in IAV-infected lymphocyte-deficient mice. (A) Relative expression of chemokine and chemokine receptor genes, measured by microarray analysis in uninfected $Rag1^{-/-}$ control mice (control) and 15 days following PR8 infection of $Rag1^{-/-}$ mice, in the presence (PR8 + Treg) or absence (PR8) of adoptively transferred Treg cells. Only genes whose expression changed significantly ($P \leq 0.05$) by more than 2-fold in PR8-infected groups compared to that of the uninfected control group are included. Asterisks in the PR8 + Treg plot denote the chemokine genes whose expression changed significantly ($P \leq 0.05$) between the PR8 and the PR8 + Treg groups. (B) Fold change in $Ccl8$ transcription in the lungs of PR8-infected $Rag1^{-/-}$ mice with (PR8 + Treg) or without (PR8) transferred Treg cells before (days 15 to 19) and during (days 20 to 26) the appearance of severe clinical disease in PR8-infected $Rag1^{-/-}$ recipients of Treg cells. Plots show the mean (± standard errors of the mean [SEM]) values of three to eight mice per group per time point. (C) Immunofluorescent detection of CCL8 (*blue*) in the lungs of uninfected $Rag1^{-/-}$ control mice (control) and 14 days following PR8 infection of $Rag1^{-/-}$ mice in the presence (PR8 + Treg) or absence (PR8) of adoptively transferred Treg cells. Lung sections were counterstained with Hoechst (red) to reveal cell nuclei and are representative of two to four mice per group. (D) Levels of CCL8/MCP-2 measured in the sera of uninfected $Rag1^{-/-}$ control mice (control) or PR8-infected $Rag1^{-/-}$ mice with (PR8 + Treg) or without (PR8) transferred Treg cells. Plots show the mean (±SEM) values of 5 to 14 mice per group. (E) Levels of CCL2/MCP-1 measured in the sera of uninfected $Rag1^{-/-}$ control mice (control) or PR8-infected $Rag1^{-/-}$ mice with (PR8 + Treg) or without (PR8) transferred Treg cells. Plots show the mean (±SEM) values of 5 to 12 mice per group.

gand 8 (*CCL8*), also known as monocyte chemotactic protein-2 (MCP-2), were found in higher abundance than those for any other cytokine/chemokine in the lungs of PR8-infected $Rag1^{-/-}$ mice (Fig. 6A; also see Table S1 in the supplemental material). The comparison between PR8-infected $Rag1^{-/-}$ mice that had received Treg cells and those that did not revealed that Treg cell transfer significantly affected the expression of only approximately 75 genes (see Table S2 in the supplemental material). Importantly, *Ccl8* induction by IAV infection was substantially suppressed by Treg cells (Fig. 6A). Furthermore, this suppression was specific for *Ccl8* and one other chemokine, chemokine (C-X-C motif) ligand 13 (*Cxcl13*), as Treg cell transfer did not significantly affect the induction of any other chemokine detected in PR8-infected lungs (Fig. 6A). The effect of Treg cells on *Ccl8* gene expression in the lungs of

PR8-infected mice was further validated with qRT-PCR analysis, which revealed that at early time points (days 15 to 19) Treg cells suppressed the induction of *Ccl8* transcription by PR8 infection to levels comparable to those seen in uninfected mice (Fig. 6B). However, *Ccl8* transcription was strongly induced in the lungs of PR8-infected $Rag1^{-/-}$ mice at later time points (days 20 to 26) independently of the presence of Treg cells (Fig. 6B). Moreover, CCL8/MCP-2 protein expression was readily detected in inflammatory lesions of PR8-infected but not uninfected lungs 14 days postinfection, and it was reduced at this early time point by the adoptive transfer of Treg cells (Fig. 6C). Thus, Treg cells delayed, but did not prevent, the induction of *Ccl8* expression during IAV infection. Another monocytic chemotactic protein, which has properties overlapping those of CCL8/MCP-2 and which has been impli-

cated in the recruitment of monocytes/macrophages into the lungs of IAV-infected mice (1, 32), is CCL2, also known as MCP-1. *Ccl2* expression was induced in the lungs of PR8-infected *Rag1*$^{-/-}$ mice compared to results for the uninfected controls (Fig. 6A; also see Table S1 in the supplemental material) but was not affected by the transfer of Treg cells (Fig. 6A; also see Table S2 in the supplemental material). Similarly, serum levels of CCL2/MCP-1 were strongly upregulated by PR8 infection and were not affected by Treg cells (Fig. 6E). In contrast, serum levels of CCL8/MCP-2 were readily detectable in uninfected controls and were unaffected by either PR8 infection or Treg cell transfer (Fig. 6D). Thus, the effect of Treg cells on chemokine expression appeared to be specific for CCL8/MCP-2 and for the lung tissue. These results also highlight the fact that local changes in inflammatory or chemotactic factors may not always be faithfully represented by changes seen in the circulation.

Treg cells and antibodies provide weight loss-free resolution of IAV infection. Although Treg cells were able to delay the induction of *Ccl8* expression, suppress lung monocytosis, and prolong survival following the PR8 infection of *Rag1*$^{-/-}$ mice, they were unable to prevent the ultimate development of severe pathology and death. Lung monocytosis was reduced by Treg cells in PR8-infected *Rag1*$^{-/-}$ recipients compared to levels for controls, even at time points when these recipients experienced clinical symptoms comparable to those of controls (Fig. 5A). As Treg cell transfer had no impact on viral replication (Fig. 2D), it was possible that the ensuing pathology in the presence of Treg cells was directly caused by the virus. To address this question, we examined the effect of Treg cell transfer in partially immunodeficient mice that could control IAV replication. T-cell-deficient C-*Foxn1*^{nu} (nude) mice are able to mount a T-cell-independent neutralizing antibody response to IAV and do survive a low-dose PR8 infection (26). Importantly, whereas C-*Foxn1*^{nu} control mice displayed the expected pattern of body weight loss, an indication of clinical pathology, following PR8 infection, C-*Foxn1*^{nu} mice that received Treg cells were virtually disease free, and their body weights did not change significantly (Fig. 7A). The disease-preventing effect of Treg cell transfer was not mediated by the enhancement of the T-cell-independent neutralizing antibody response in recipient mice. Whereas virus-neutralizing serum antibodies were not detected in C-*Foxn1*^{nu} mice prior to PR8 infection, these mice mounted an antibody response of neutralizing activity similar to that of wild-type control mice 6 days after PR8 infection (Fig. 7B) (26). The transfer of Treg cells into PR8-infected C-*Foxn1*^{nu} mice led to a significant suppression of this early T-cell-independent antibody response (Fig. 7B). On day 12 after PR8 infection, when wild-type mice showed a strong T-cell-dependent antibody response, neutralizing antibody titers were comparably low in C-*Foxn1*^{nu} mice whether or not they had received Treg cells (Fig. 7B). Thus, Treg cells exerted transient suppression instead of the enhancement of the T-cell-independent antibody response of C-*Foxn1*^{nu} mice to IAV infection. Taken together, these results indicate that the combined effect of Treg cells, likely acting on innate immunity, together with the neutralizing effect of T-cell-independent antibodies were able to prevent clinical symptoms of IAV infection.
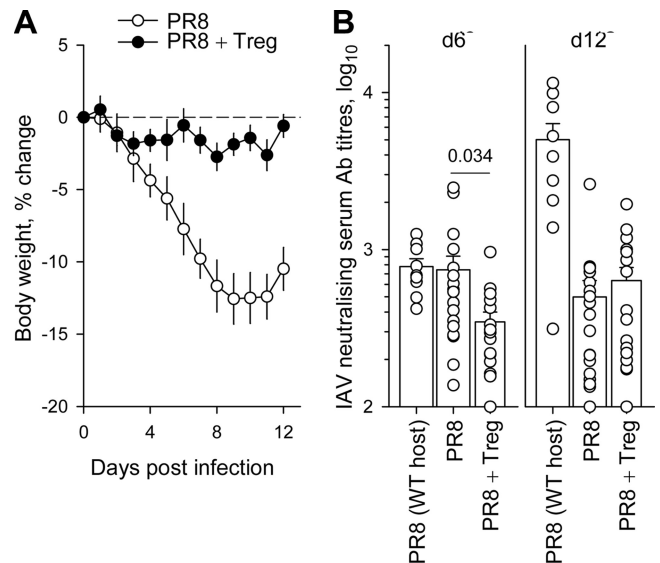

FIG. 7. Clinical disease-free course of IAV infection in T-cell-deficient recipients of Treg cells. (A) Changes in body weight of PR8-infected C-*Foxn1*^{nu} mice in the presence (PR8 + Treg) or absence (PR8) of adoptively transferred Treg cells. Lines show the mean ($\pm$ standard errors of the mean) values of 9 to 13 mice per group from three independent experiments. $P < 0.006$ from day 6 until the end of the experiment. (B) Serum titers of PR8-neutralizing antibodies in wild-type control mice (PR8 [WT host]) or C-*Foxn1*^{nu} mice with (PR8 + Treg) or without (PR8) transferred Treg cells measured 6 or 12 days after PR8 infection. Each symbol represents an individual mouse. No neutralizing antibodies were detected at these serum dilutions in either wild-type or C-*Foxn1*^{nu} mice prior to PR8 infection.

DISCUSSION

It is thought that both immune-mediated and virus-mediated effects contribute to the pathogenesis of IAV infection, although the extent of each contribution may vary depending on host and viral characteristics (36, 44, 62). The results of our experiments with the PR8 infection of lymphocyte-deficient mice revealed that a substantial amount of pathology could be delayed or prevented by the adoptive transfer of Treg cells, and therefore it was mediated by a host response other than the adaptive immune response.

The infection of lymphocyte-deficient *Rag1*$^{-/-}$ mice provided a window of opportunity for the study of the innate immune response to IAV. In immunologically naïve wild-type hosts, this response would correspond to the early innate phase of infection, which may be accompanied by particularly rapid disease development, especially following infection with highly pathogenic IAVs (5, 8, 44, 45). PR8-infected *Rag1*$^{-/-}$ mice displayed a moderately protracted course of disease, with clinical symptoms starting on day 7 postinfection and progressively worsening for an average of 10 days before mice reached the endpoint of clinical disease. This relatively late appearance of clinical disease was due in part to the omission of anesthesia from the experimental protocol, such that the infection was initiated in the upper respiratory track and spread only to the lung via natural virus replication (69). Indeed, the PR8 infection of anesthetized *Rag1*$^{-/-}$ mice led to the appearance of clinical symptoms by day 2 postinfection, with an average survival time

of approximately 8 days (data not shown). Treg cell transfer into $Rag1^{-/-}$ mice infected under anesthesia failed to delay the rapid disease development (data not shown), likely due to the limited number of FACS-purified Treg cells that we were able to transfer into these recipients (approximately 30 times less than the number of Treg cells found in wild-type mice). Indeed, Treg cells transferred into $Rag1^{-/-}$ mice infected without anesthesia accumulated in the lungs after 3 weeks to an average of 0.12×10^4 FoxP3$^+$ Treg cells per mouse, whereas we have found that the peak number of FoxP3$^+$ Treg cells that accumulated in the lungs of wild-type mice 7 days after PR8 infection (on average, 0.42×10^4) was approximately three times higher. Another potential difference in the response of $Rag1^{-/-}$ or C-$Foxn1^{nu}$ mice from that of wild-type mice is the state of innate immune reactivity, which has been suggested to be heightened in the absence of T cells (13). However, the number of monocytes/macrophages in the lungs of PR8-infected $Rag1^{-/-}$ mice was comparable to that of the same cells in the lungs of PR8-infected wild-type mice (on average, 1.14×10^6 CD11b$^+$ F4/80$^+$ cells per mouse; $n = 3$) and also to what has been reported previously (1, 32). Furthermore, the transfer of Treg-depleted CD4$^+$ T cells into C-$Foxn1^{nu}$ mice (26) and of Treg-depleted naïve CD4$^+$ T cells into $Rag1^{-/-}$ mice (in the present study) have been shown to exacerbate clinical pathology following PR8 infection. Although it currently is unclear whether CD4$^+$ T cells enhance pathology directly or through effects on innate immunity, these results emphasize that the host response to IAV is not necessarily more extreme in $Rag1^{-/-}$ or C-$Foxn1^{nu}$ mice compared to that of wild-type mice. Lastly, PR8-induced pathology in mice doubly deficient in Rag1 and the IL-2 receptor gamma chain ($Rag1^{-/-}$ $Il2rg^{-/-}$ mice lacking T, B, and NK cells) was not significantly different from that in $Rag1^{-/-}$ mice (data not shown), arguing against a major involvement of NK cells in this process.

It is generally thought that lung damage represents the underlying pathology leading to the development of clinical disease in IAV infection (10). However, IAV has the potential to disseminate at and/or replicate in sites other than the lungs, which also could contribute to clinical disease. For example, infectious IAV has been isolated from the lung-draining lymph nodes, heart, or thymus of wild-type mice infected with PR8 (15, 22), the heart and spleen of macaques infected with a reconstructed 1918 virus (28), and the intestine or serum of humans infected with H5N1 IAV (10, 64), suggesting that viremia can occur. PR8-infected $Rag1^{-/-}$ mice did show the systemic presence of the virus, which were determined by levels of PR8 *matrix* mRNA. However, our inability to isolate infectious virus from any location other than the lungs suggested that the systemic dissemination of viral RNA was not associated with high-level replication. Instead, the systemic presence of viral RNA could indicate the migration of immune cells, including macrophages and dendritic cells, which are known to be infected by IAV and which may not support virus production (43, 45, 54). Indeed, viral RNA was found to be more widely distributed than infectious virus in previous studies (15). Furthermore, the parenteral administration of PR8 to $Rag1^{-/-}$ mice resulted in a pattern of viral RNA distribution and the onset of clinical disease similar to those induced by intranasal infection. As previously shown (16), this apparent restriction of PR8 replication in lungs of $Rag1^{-/-}$ mice likely was related to the relative paucity of proteases that can mediate the cleavage and activation of PR8 hemagglutinin in extrapulmonary tissues. Our subsequent analysis of the pathogenic mechanism of IAV infection and its potential suppression by Treg cells therefore was concentrated in the lungs.

The most profound change in the lungs of PR8-infected $Rag1^{-/-}$ mice, revealed by microarray analysis and supported by histological and flow-cytometric findings, was the overabundance of monocytes/macrophages, which was characterized by the expression of CD11b, Ly-6C, and F4/80 (4, 55). Whereas they represented a minor population in uninfected organs, these myeloid cells accounted for the highest percentage of mononuclear cells isolated from the infected lungs. However, monocytes/macrophages may have been enriched, to some extent, by the procedure used for their isolation, which involved density gradient centrifugation. Indeed, neutrophils also were present at elevated numbers in the lungs of PR8-infected $Rag1^{-/-}$ mice and were visible is histological sections. Nevertheless, monocytes/macrophages still were the most abundant cell type in noncentrifuged cell suspensions from infected lungs (data not shown), and our microarray analysis of total infected lung tissue confirmed the overrepresentation of monocyte/macrophage-specific gene transcripts compared to those of other bone marrow-derived cell types. Our findings are in line with previous studies, which have reported the increased influx of myeloid cells into the lungs following IAV infection (1, 25, 32, 45, 63). Using both less-pathogenic PR8 and X31 viruses and highly pathogenic H5N1 and 1918 viruses, these studies also have positively correlated the extent of myeloid cell accumulation in the lungs with the pathogenicity of the infecting virus (1, 25, 32, 45, 63). It thus is highly likely that this early and pronounced accumulation of myeloid cells in IAV-infected lungs is a significant contributor to lung pathology and clinical disease. Importantly, this particular event in IAV pathogenesis appears to be the target of Treg cell suppression in our adoptive transfer model.

Our experiments revealed a significant suppressive effect of Treg cell transfer into PR8-infected $Rag1^{-/-}$ mice on monocyte/macrophage accumulation in the lungs, which was accompanied by a delay in clinical disease. The analysis of FoxP3 expression in adoptively transferred cells showed a progressive accumulation of FoxP3$^-$ CD4$^+$ T cells with time in PR8-infected $Rag1^{-/-}$ recipients. These FoxP3$^-$ CD4$^+$ T cells may have resulted from the preferential expansion of FoxP3$^-$ precursors already present in the initial population prior to transfer, as this population was selected on the basis of CD25 expression and contained a significant fraction (up to 8%) of FoxP3$^-$ CD4$^+$ T cells. Alternatively, they could be the result of the conversion of FoxP3$^+$ Treg cells into FoxP3$^-$ CD4$^+$ effector T cells, a phenomenon that has been reported to occur under these experimental conditions (14, 29, 71). Indeed, at the end of the observation period, the percentage of FoxP3$^+$ Treg cells in total CD4$^+$ T cells reached a minimum of just more than 30% in the lung and 80% in the spleen. Nevertheless, this minimum percentage of FoxP3$^+$ Treg cells still was considerably higher than their maximum percentage in either the lungs or the spleen of PR8-infected wild-type mice at any time point (data not shown). Furthermore, our results also showed that the adoptive transfer of naïve CD25$^-$ CD44^{low}

(>90% FoxP3$^-$) CD4$^+$ T cells into PR8-infected $Rag1^{-/-}$ mice had a disease-accelerating effect, in contrast to the transfer of CD25$^+$ Treg cells, which had the opposite effect. Similarly, we have previously shown that the transfer of naïve (CD25$^-$ CD44^{low}) or memory (CD25$^-$CD44^{high}) CD4$^+$ T cells from IAV-immune donor mice into IAV-infected C-$Foxn1^{nu}$ recipients led to the enhancement of clinical disease (26), highlighting the pathogenic potential of effector CD4$^+$ T cells during IAV infection. Therefore, the suppression of clinical disease upon the transfer of CD25$^+$ Treg cells into PR8-infected $Rag1^{-/-}$ mice is unlikely to be mediated by FoxP3$^-$ CD4$^+$ effector T cells. Instead, the presence of FoxP3$^-$ CD4$^+$ effector T cells, which potentially contribute to IAV pathogenesis in these recipient mice, emphasizes the disease-suppressive effect of Treg cells. Indeed, our data indicate that FoxP3$^+$ Treg cells would have to suppress both innate immune-mediated pathology and any potential pathogenic contribution of FoxP3$^-$ CD4$^+$ effector T cells to ameliorate the clinical symptoms of their $Rag1^{-/-}$ or C-$Foxn1^{nu}$ adoptive hosts to a significant degree compared to that of $Rag1^{-/-}$ or C-$Foxn1^{nu}$ mice that did not receive any T cells.

The potential of suppressor T cells to prevent clinical disease following IAV infection had been suspected almost as early as the demonstration of the pathogenic role of effector T cells in this infection in at least one study published in the suppressor T-cell era (31). However, with the demise of the suppressor T-cell concept during recent decades, the role of Treg cells in IAV infection and, more specifically, their mechanism of action, remained unexplored. More-recent studies have implicated Treg cells in impairing the induction of CD8$^+$ T cells by IAV vaccination (18) and of CD4$^+$ T cell memory by IAV infection specifically in IL-6-deficient mice (34). However, a potential involvement of Treg cells in the development of IAV-induced pathology was not investigated. Our present study demonstrates that Treg cells influenced the chemotactic properties of IAV-infected lungs, which is likely to be mechanistically linked to the reduced accumulation of myeloid cells and the amelioration of IAV-induced pathology. Surprisingly, the observed suppressive effect of Treg cells was highly specific for the expression of $Ccl8$ and $Cxcl13$ in the lungs and did not extend to other chemotactic factors. CXCL13 displays a well-characterized chemotactic activity for CXCR5-expressing B cells and follicular helper T cells (42). Although CXCL13 induction by IAV and its suppression by Treg cells may influence the development of immunity or pathology in wild-type mice (41), this chemokine is unlikely to be involved in IAV-induced pathology in $Rag1^{-/-}$ mice, given the absence of CXCL13 targets (T and B cells) in these mice. In contrast, the monocyte chemoattractant CCL8/MCP-2 could be centrally involved, and indeed, Treg cells significantly delayed its induction by IAV infection in lung tissue.

CCL8/MCP-2 belongs to a family of chemokines that mediate leukocyte recruitment into inflamed tissues (11, 46, 55, 58). It shares certain chemotactic properties with other MCPs, partly as a result of common signaling receptors (11, 46, 55, 58). Together with a host of other inflammatory mediators, $Ccl8$ transcription has been reported to be strongly induced in the lung of mice (25) or the bronchi of macaques (8) infected with highly pathogenic IAVs, and these findings are supported by our observations. In addition to CCL8/MCP-2, the induc-tion of CCL2/MCP-1 also has been seen in the lungs of mice (25, 45) and in sera of humans and macaques (10, 28) infected with highly pathogenic IAVs. Similarly, we have found that serum levels of MCP-1, IL-6, and CXCL10/IP-10 were highly elevated following the PR8 infection of $Rag1^{-/-}$ mice, although the transfer of Treg cells had no measurable effect on their induction (data not shown). An additional level of complexity stems from the utilization of shared chemokine receptors by various MCPs. For example, both CCL2/MCP-1 and CCL8/MCP-2, as well as other MCPs, bind to CCR2 (55). Studies of the PR8 infection of CCR2-deficient mice have yielded conflicting results (1, 32), possibly due to differences in experimental protocols. In addition to CCR2, CCL2/MCP-1 and CCL8/MCP-2 bind unique receptors (11, 46, 55, 58), which may mediate the nonoverlapping functions of these two MCPs. Although defining the precise role of MCPs in IAV pathogenesis will require further investigation, taken together these studies highlight a potentially important contribution of MCPs to IAV-associated pathology. The involvement of MCPs in IAV pathogenesis also is supported by the fact that the pharmacological inhibition of MCP production has been reported to ameliorate the severity of IAV infection (1). Moreover, the regulation of MCP production by Treg cells also has been suggested by observations made in other systems. The depletion of Treg cells in a mouse model for RSV infection was associated with the elevated production of CCL2/MCP-1, delayed viral clearance, and changes in the pattern of pathology (50). Moreover, Treg cell ablation during HSV-2 infection led to the enhanced production of CCL2/MCP-1 in the lymph nodes (35). MCPs are known to be produced by a variety of cell types (11, 46, 58), and a question that has remained unanswered in previously published studies and in the current study is precisely how Treg cells regulate MCP induction. For example, fibroblasts, epithelial cells, and airway smooth-muscle cells are among the cell types that have been reported to produce CCL8/MCP-2 (47, 60), and they could be directly or indirectly suppressed by Treg cells.

Treg cell-mediated delay in the induction of $Ccl8$ following IAV infection is consistent with both the reduced accumulation and altered distribution of monocytes/macrophages in the lungs of infected $Rag1^{-/-}$ mice. However, the precise Treg cell-produced mediator of these effects has not been revealed in our current study. Although several studies support a role for Treg cell-produced IL-10 in the suppression of inflammatory pathology in other contexts (2, 9, 19, 23, 27, 44, 49), our results with Treg cells deficient in IL-10 production have not indicated a similar requirement in the suppression of PR8-induced pathology in $Rag1^{-/-}$ mice. Two recent studies also have supported a role for IL-10 specifically in IAV pathogenesis, although in both of these studies effector T cells, rather than Treg cells, were the main contributors of IL-10 production (38, 61). One study demonstrated the IL-10-dependent suppression of lung inflammation and pathology following IAV infection (61). The blockade of IL-10 in this study led to increased mortality and accelerated death following IAV infection (61). In contrast, the other study has implicated IL-10 in the suppression of a protective CD4$^+$ T-cell response to IAV and showed that the lack of IL-10 decreased mortality and delayed death following lethal IAV infection, whereas no effect of IL-10 could be demonstrated following sublethal IAV in-

fection (38). Taken together, these studies suggest that effector T-cell-derived IL-10 is harmful, neutral, or beneficial in the host response to IAV infection, depending on many ill-defined parameters. Nevertheless, our results indicated that Treg cell-derived IL-10 was dispensable in the suppression of innate pathology by Treg cells following the PR8 infection of $Rag1^{-/-}$ mice. Similarly, whereas a crucial contribution of IL-35 in the suppression of T-cell-driven pathology has been suggested by one study (9), we were unable to demonstrate any requirement for Treg cell-produced IL-35 in this system. In addition to the production of IL-10 and IL-35, Treg cells have been shown to use various other mediators for their suppression (56, 65). Precisely which of these mediators, in isolation or in combination, contribute to the suppression of innate immune pathology in IAV mice by Treg cells will require further study.

It is important to note that although the adoptive transfer of Treg cells into PR8-infected $Rag1^{-/-}$ mice significantly delayed the onset of pathology and clinical symptoms, it did not prevent the eventual development of severe pathology and disease in these mice. Therefore, additional pathogenic mechanisms, which are not influenced by the suppressive activity of Treg cells, also may contribute to the overall pathology associated with IAV infection. PR8 continued to replicate in the lungs of $Rag1^{-/-}$ mice at very high levels regardless of the presence of Treg cells. This finding emphasized that at least part of the pathology of IAV infection can be suppressed by Treg cells despite the presence of very high virus levels and thus should be innate immune mediated. It also suggested that unabated IAV replication was responsible for the part of the pathogenesis that was not suppressed by Treg cells. This hypothesis was strongly supported by our findings following Treg cell transfer into C-$Foxn1^{nu}$ mice, which remained virtually disease free following PR8 infection. In these mice, the combination of Treg cells, suppressing innate immune pathology, and virus-neutralizing antibodies, reducing virus-induced pathology, likely blocked both major contributors of pathogenesis during IAV infection. Therefore, our study suggested that the simultaneous targeting of both innate immune reactivity and virus replication will prove more beneficial in the treatment of IAV infection-induced pathology.

ACKNOWLEDGMENTS

REFERENCES

1. Aldridge, J. R., Jr., C. E. Moseley, D. A. Boltz, N. J. Negovetich, C. Reynolds, J. Franks, S. A. Brown, P. C. Doherty, R. G. Webster, and P. G. Thomas. 2009. TNF/iNOS-producing dendritic cells are the necessary evil of lethal influenza virus infection. Proc. Natl. Acad. Sci. U. S. A. 106:5306–5311.
2. Annacker, O., R. Pimenta-Araujo, O. Burlen-Defranoux, T. C. Barbosa, A. Cumano, and A. Bandeira. 2001. CD25+ CD4+ T cells regulate the expansion of peripheral CD4 T cells through the production of IL-10. J. Immunol. 166:3008–3018.
3. Antunes, I., M. Tolaini, A. Kissenpfennig, M. Iwashiro, K. Kuribayashi, B. Malissen, K. Hasenkrug, and G. Kassiotis. 2008. Retrovirus-specificity of

regulatory T cells is neither present nor required in preventing retrovirus-induced bone marrow immune pathology. Immunity 29:782–794.
4. Auffray, C., M. H. Sieweke, and F. Geissmann. 2009. Blood monocytes: development, heterogeneity, and relationship with dendritic cells. Annu. Rev. Immunol. 27:669–692.
5. Baskin, C. R., H. Bielefeldt-Ohmann, T. M. Tumpey, P. J. Sabourin, J. P. Long, A. Garcia-Sastre, A. E. Tolnay, R. Albrecht, J. A. Pyles, P. H. Olson, L. D. Aicher, E. R. Rosenzweig, K. Murali-Krishna, E. A. Clark, M. S. Kotur, J. L. Fornek, S. Proll, R. E. Palermo, C. L. Sabourin, and M. G. Katze. 2009. Early and sustained innate immune response defines pathology and death in nonhuman primates infected by highly pathogenic influenza virus. Proc. Natl. Acad. Sci. U. S. A. 106:3455–3460.
6. Belkaid, Y., and K. Tarbell. 2009. Regulatory T cells in the control of host-microorganism interactions. Annu. Rev. Immunol. 27:551–589.
7. Cameron, M. J., J. F. Bermejo-Martin, A. Danesh, M. P. Muller, and D. J. Kelvin. 2008. Human immunopathogenesis of severe acute respiratory syndrome (SARS). Virus Res. 133:13–19.
8. Cilloniz, C., K. Shinya, X. Peng, M. J. Korth, S. C. Proll, L. D. Aicher, V. S. Carter, J. H. Chang, D. Kobasa, F. Feldmann, J. E. Strong, H. Feldmann, Y. Kawaoka, and M. G. Katze. 2009. Lethal influenza virus infection in macaques is associated with early dysregulation of inflammatory related genes. PLoS Pathog. 5:e1000604.
9. Collison, L. W., C. J. Workman, T. T. Kuo, K. Boyd, Y. Wang, K. M. Vignali, R. Cross, D. Sehy, R. S. Blumberg, and D. A. A. Vignali. 2007. The inhibitory cytokine IL-35 contributes to regulatory T-cell function. Nature 450:566–569.
10. de Jong, M. D., C. P. Simmons, T. T. Thanh, V. M. Hien, G. J. Smith, T. N. Chau, D. M. Hoang, N. V. Chau, T. H. Khanh, V. C. Dong, P. T. Qui, B. V. Cam, d. Q. Ha, Y. Guan, J. S. Peiris, N. T. Chinh, T. T. Hien, and J. Farrar. 2006. Fatal outcome of human influenza A (H5N1) is associated with high viral load and hypercytokinemia. Nat. Med. 12:1203–1207.
11. Deshmane, S. L., S. Kremlev, S. Amini, and B. E. Sawaya. 2009. Monocyte chemoattractant protein-1 (MCP-1): an overview. J. Interferon Cytokine Res. 29:313–326.
12. Dittmer, U., H. He, R. J. Messer, S. Schimmer, A. R. M. Olbrich, C. Ohlen, P. D. Greenberg, I. M. Stromnes, M. Iwashiro, and S. Sakaguchi. 2004. Functional impairment of CD8+ T cells by regulatory T cells during persistent retroviral infection. Immunity 20:293–303.
13. Dong Kim, K., J. Zhao, S. Auh, X. Yang, P. Du, H. Tang, and Y. X. Fu. 2007. Adaptive immune cells temper initial innate responses. Nat. Med. 13:1248–1252.
14. Duarte, J. H., S. Zelenay, M. L. Bergman, A. C. Martins, and J. Demengeot. 2009. Natural Treg cells spontaneously differentiate into pathogenic helper cells in lymphopenic conditions. Eur. J. Immunol. 39:948–955.
15. Fislová, T., M. Gocnik, T. Sladkova, V. Durmanova, J. Rajcani, E. Vareckova, V. Mucha, and F. Kostolansky. 2009. Multiorgan distribution of human influenza A virus strains observed in a mouse model. Arch. Virol. 154:409–419.
16. García-Sastre, A., R. K. Durbin, H. Zheng, P. Palese, R. Gertner, D. E. Levy, and J. E. Durbin. 1998. The role of interferon in influenza virus tissue tropism. J. Virol. 72:8550–8558.
17. Guidotti, L. G., and F. V. Chisari. 2006. Immunobiology and pathogenesis of viral hepatitis. Annu. Rev. Pathol. 1:23–61.
18. Haeryfar, S. M. M., R. J. DiPaolo, D. C. Tscharke, J. R. Bennink, and J. W. Yewdell. 2005. Regulatory T cells suppress CD8+ T cell responses induced by direct priming and cross-priming and moderate immunodominance disparities. J. Immunol. 174:3344–3351.
19. Hara, M., C. I. Kingsley, M. Niimi, S. Read, S. E. Turvey, A. R. Bushell, P. J. Morris, F. Powrie, and K. J. Wood. 2001. IL-10 is required for regulatory T cells to mediate tolerance to alloantigens in vivo. J. Immunol. 166:3789–3796.
20. Hedrick, S. M. 2004. The acquired immune system: a vantage from beneath. Immunity 21:607–615.
21. Iwashiro, M., R. J. Messer, K. E. Peterson, I. M. Stromnes, T. Sugie, and K. J. Hasenkrug. 2001. Immunosuppression by CD4+ regulatory T cells induced by chronic retroviral infection. Proc. Natl. Acad. Sci. U. S. A. 98:9226–9230.
22. Jelley-Gibbs, D. M., D. M. Brown, J. P. Dibble, L. Haynes, S. M. Eaton, and S. L. Swain. 2005. Unexpected prolonged presentation of influenza antigens promotes CD4 T cell memory generation. J. Exp. Med. 202:697–706.
23. Joetham, A., K. Takada, C. Taube, N. Miyahara, S. Matsubara, T. Koya, Y. H. Rha, A. Dakhama, and E. W. Gelfand. 2007. Naturally occurring lung CD4+CD25+ T cell regulation of airway allergic responses depends on IL-10 induction of TGF-beta. J. Immunol. 178:1433–1442.
24. Kägi, D., B. Ledermann, K. Burki, R. M. Zinkernagel, and H. Hengartner. 1996. Molecular mechanisms of lymphocyte-mediated cytotoxicity and their role in immunological protection and pathogenesis in vivo. Annu. Rev. Immunol. 14:207–232.
25. Kash, J. C., T. M. Tumpey, S. C. Proll, V. Carter, O. Perwitasari, M. J. Thomas, C. F. Basler, P. Palese, J. K. Taubenberger, A. Garcia-Sastre, D. E. Swayne, and M. G. Katze. 2006. Genomic analysis of increased host immune

and cell death responses induced by 1918 influenza virus. Nature **443:**578–581.

26. **Kassiotis, G., D. Gray, Z. Kiafard, J. Zwirner, and B. Stockinger.** 2006. Functional specialization of memory Th cells revealed by expression of integrin CD49b. J. Immunol. **177:**968–975.

27. **Kearley, J., J. E. Barker, D. S. Robinson, and C. M. Lloyd.** 2005. Resolution of airway inflammation and hyperreactivity after in vivo transfer of CD4+CD25+ regulatory T cells is interleukin 10 dependent. J. Exp. Med. **202:**1539–1547.

28. **Kobasa, D., S. M. Jones, K. Shinya, J. C. Kash, J. Copps, H. Ebihara, Y. Hatta, J. Hyun Kim, P. Halfmann, M. Hatta, F. Feldmann, J. B. Alimonti, L. Fernando, Y. Li, M. G. Katze, H. Feldmann, and Y. Kawaoka.** 2007. Aberrant innate immune response in lethal infection of macaques with the 1918 influenza virus. Nature **445:**319–323.

29. **Komatsu, N., M. E. Mariotti-Ferrandiz, Y. Wang, B. Malissen, H. Waldmann, and S. Hori.** 2009. Heterogeneity of natural Foxp3+ T cells: a committed regulatory T-cell lineage and an uncommitted minor population retaining plasticity. Proc. Natl. Acad. Sci. U. S. A. **106:**1903–1908.

30. **Lanteri, M. C., K. M. O'Brien, W. E. Purtha, M. J. Cameron, J. M. Lund, R. E. Owen, J. W. Heitman, B. Custer, D. F. Hirschkorn, L. H. Tobler, N. Kiely, H. E. Prince, L. C. Ndhlovu, D. F. Nixon, H. T. Kamel, D. J. Kelvin, M. P. Busch, A. Y. Rudensky, M. S. Diamond, and P. J. Norris.** 2009. Tregs control the development of symptomatic West Nile virus infection in humans and mice. J. Clin. Investig. **119:**3266–3277.

31. **Liew, F. Y., and S. M. Russell.** 1983. Inhibition of pathogenic effect of effector T cells by specific suppressor T cells during influenza virus infection in mice. Nature **304:**541–543.

32. **Lin, K. L., Y. Suzuki, H. Nakano, E. Ramsburg, and M. D. Gunn.** 2008. CCR2+ monocyte-derived dendritic cells and exudate macrophages produce influenza-induced pulmonary immune pathology and mortality. J. Immunol. **180:**2562–2572.

33. **Littman, D. R., and A. Y. Rudensky.** 2010. Th17 and regulatory T cells in mediating and restraining inflammation. Cell **140:**845–858.

34. **Longhi, M. P., K. Wright, S. N. Lauder, M. A. Nowell, G. W. Jones, A. J. Godkin, S. A. Jones, and A. M. Gallimore.** 2008. Interleukin-6 is crucial for recall of influenza-specific memory CD4+ T cells. PLoS Pathog. **4:**e1000006.

35. **Lund, J. M., L. Hsing, T. T. Pham, and A. Y. Rudensky.** 2008. Coordination of early protective immunity to viral infection by regulatory T cells. Science **320:**1220–1224.

36. **Maines, T. R., K. J. Szretter, L. Perrone, J. A. Belser, R. A. Bright, H. Zeng, T. M. Tumpey, and J. M. Katz.** 2008. Pathogenesis of emerging avian influenza viruses in mammals and the host innate immune response. Immunol. Rev. **225:**68–84.

37. **Maloy, K. J., L. Salaun, R. Cahill, G. Dougan, N. J. Saunders, and F. Powrie.** 2003. CD4+ CD25+ TR cells suppress innate immune pathology through cytokine-dependent mechanisms. J. Exp. Med. **197:**111–119.

38. **McKinstry, K. K., T. M. Strutt, A. Buck, J. D. Curtis, J. P. Dibble, G. Huston, M. Tighe, H. Hamada, S. Sell, R. W. Dutton, and S. L. Swain.** 2009. IL-10 deficiency unleashes an influenza-specific Th17 response and enhances survival against high-dose challenge. J. Immunol. **182:**7353–7363.

39. **Mombaerts, P., J. Iacomini, R. S. Johnson, K. Herrup, S. Tonegawa, and V. E. Papaioannou.** 1992. RAG-1-deficient mice have no mature B and T lymphocytes. Cell **68:**869–877.

40. **Moskophidis, D., and D. Kioussis.** 1998. Contribution of Virus-specific CD8+ cytotoxic T cells to virus clearance or pathologic manifestations of influenza virus infection in a T cell receptor transgenic mouse model. J. Exp. Med. **188:**223–232.

41. **Moyron-Quiroz, J. E., J. Rangel-Moreno, K. Kusser, L. Hartson, F. Sprague, S. Goodrich, D. L. Woodland, F. E. Lund, and T. D. Randall.** 2004. Role of inducible bronchus associated lymphoid tissue (iBALT) in respiratory immunity. Nat. Med. **10:**927–934.

42. **Müller, G., U. E. Hopken, and M. Lipp.** 2003. The impact of CCR7 and CXCR5 on lymphoid organ development and systemic immunity. Immunol. Rev. **195:**117–135.

43. **Nimmerjahn, F., D. Kobelt, A. Steinkasserer, A. Menke, G. Hobom, U. Behrends, G. W. Bornkamm, and J. Mautner.** 2003. Efficient generation and expansion of antigen-specific CD4+ T cells by recombinant influenza viruses. Eur. J. Immunol. **33:**3331–3341.

44. **Peiris, J. S. M., C. Y. Cheung, C. Y. H. Leung, and J. M. Nicholls.** 2009. Innate immune responses to influenza A H5N1: friend or foe? Trends Immunol. **30:**574–584.

45. **Perrone, L. A., J. K. Plowden, A. Garcia-Sastre, J. M. Katz, and T. M. Tumpey.** 2008. H5N1 and 1918 pandemic influenza virus infection results in early and excessive infiltration of macrophages and neutrophils in the lungs of mice. PLoS Pathog. **4:**e1000115.

46. **Proost, P., A. Wuyts, and J. Van Damme.** 1996. Human monocyte chemotactic proteins-2 and -3: structural and functional comparison with MCP-1. J. Leukoc. Biol. **59:**67–74.

47. **Pype, J. L., L. J. Dupont, P. Menten, E. Van Coillie, G. Opdenakker, J. Van Damme, K. Fan Chung, M. G. Demedts, and G. M. Verleden.** 1999. Expression of monocyte chemotactic protein (MCP)-1, MCP-2, and MCP-3 by human airway smooth-muscle cells. modulation by corticosteroids and T-helper 2 cytokines. Am. J. Respir. Cell Mol. Biol. **21:**528–536.

48. **Rouse, B. T., P. P. Sarangi, and S. Suvas.** 2006. Regulatory T cells in virus infections. Immunol. Rev. **212:**272–286.

49. **Rubtsov, Y. P., J. P. Rasmussen, E. Y. Chi, J. Fontenot, L. Castelli, X. Ye, P. Treuting, L. Siewe, A. Roers, J. Henderson, W. Muller, and A. Y. Rudensky.** 2008. Regulatory T cell-derived interleukin-10 limits inflammation at environmental interfaces. Immunity **28:**546–558.

50. **Ruckwardt, T. J., K. L. Bonaparte, M. C. Nason, and B. S. Graham.** 2009. Regulatory T cells promote early influx of CD8+ T cells in the lungs of respiratory syncytial virus-infected mice and diminish immunodominance disparities. J. Virol. **83:**3019–3028.

51. **Rudensky, A. Y., and D. J. Campbell.** 2006. In vivo sites and cellular mechanisms of T reg cell-mediated suppression. J. Exp. Med. **203:**489–492.

52. **Sakaguchi, S., T. Yamaguchi, T. Nomura, and M. Ono.** 2008. Regulatory T cells and immune tolerance. Cell **133:**775–787.

53. **Sehrawat, S., S. Suvas, P. P. Sarangi, A. Suryawanshi, and B. T. Rouse.** 2008. In vitro-generated antigen-specific CD4+ CD25+ Foxp3+ regulatory T cells control the severity of herpes simplex virus-induced ocular immunoinflammatory lesions. J. Virol. **82:**6838–6851.

54. **Seo, S. H., R. Webby, and R. G. Webster.** 2004. No apoptotic deaths and different levels of inductions of inflammatory cytokines in alveolar macrophages infected with influenza viruses. Virology **329:**270–279.

55. **Serbina, N. V., T. Jia, T. M. Hohl, and E. G. Pamer.** 2008. Monocyte-mediated defense against microbial pathogens. Annu. Rev. Immunol. **26:** 421–452.

56. **Shevach, E. M.** 2009. Mechanisms of Foxp3+ T regulatory cell-mediated suppression. Immunity **30:**636–645.

57. **Sissons, J. G., A. J. Carmichael, N. McKinney, J. H. Sinclair, and M. R. Wills.** 2002. Human cytomegalovirus and immunopathology. Springer Semin. Immunopathol. **24:**169–185.

58. **Sozzani, S., M. Locati, D. Zhou, M. Rieppi, W. Luini, G. Lamorte, G. Bianchi, N. Polentarutti, P. Allavena, and A. Mantovani.** 1995. Receptors, signal transduction, and spectrum of action of monocyte chemotactic protein-1 and related chemokines. J. Leukoc. Biol. **57:**788–794.

59. **Stockinger, B., G. Kassiotis, and C. Bourgeois.** 2004. Homeostasis and T cell regulation. Curr. Opin. Immunol. **16:**775–779.

60. **Struyf, S., E. Van Collie, L. Paemen, W. Put, J. P. Lenaerts, P. Proost, G. Opdenakker, and J. Van Damme.** 1998. Synergistic induction of MCP-1 and -2 by IL-1beta and interferons in fibroblasts and epithelial cells. J. Leukoc. Biol. **63:**364–372.

61. **Sun, J., R. Madan, C. L. Karp, and T. J. Braciale.** 2009. Effector T cells control lung inflammation during acute influenza virus infection by producing IL-10. Nat. Med. **15:**277–284.

62. **Taubenberger, J. K., and D. M. Morens.** 2008. The pathology of influenza virus infections. Annu. Rev. Pathol. **3:**499–522.

63. **Tumpey, T. M., A. Garcia-Sastre, J. K. Taubenberger, P. Palese, D. E. Swayne, M. J. Pantin-Jackwood, S. Schultz-Cherry, A. Solorzano, N. Van Rooijen, J. M. Katz, and C. F. Basler.** 2005. Pathogenicity of influenza viruses with genes from the 1918 pandemic virus: functional roles of alveolar macrophages and neutrophils in limiting virus replication and mortality in mice. J. Virol. **79:**14933–14944.

64. **Uiprasertkul, M., P. Puthavathana, K. Sangsiriwut, P. Pooruk, K. Srisook, M. Peiris, J. M. Nicholls, K. Chokephaibulkit, N. Vanprapar, and P. Auewarakul.** 2005. Influenza A H5N1 replication sites in humans. Emerg. Infect. Dis. **11:**1036–1041.

65. **Vignali, D. A., L. W. Collison, and C. J. Workman.** 2008. How regulatory T cells work. Nat. Rev. Immunol. **8:**523–532.

66. **Ward, C. L., M. H. Dempsey, C. J. Ring, R. E. Kempson, L. Zhang, D. Gor, B. W. Snowden, and M. Tisdale.** 2004. Design and performance testing of quantitative real time PCR assays for influenza A and B viral load measurement. J. Clin. Virol. **29:**179–188.

67. **Whitton, J. L.** 2002. Immunopathology during coxsackievirus infection. Springer Semin. Immunopathol. **24:**201–213.

68. **Wing, K., Y. Onishi, P. Prieto-Martin, T. Yamaguchi, M. Miyara, Z. Fehervari, T. Nomura, and S. Sakaguchi.** 2008. CTLA-4 control over Foxp3+ regulatory T cell function. Science **322:**271–275.

69. **Yetter, R. A., S. Lehrer, R. Ramphal, and P. A. Small, Jr.** 1980. Outcome of influenza infection: effect of site of initial infection and heterotypic immunity. Infect. Immun. **29:**654–662.

70. **Zelinskyy, G., K. Dietze, T. Sparwasser, and U. Dittmer.** 2009. Regulatory T cells suppress antiviral immune responses and increase viral loads during acute infection with a lymphotropic retrovirus. PLoS Pathog. **5:**e1000406.

71. **Zhou, X., S. Bailey-Bucktrout, L. T. Jeker, and J. A. Bluestone.** 2009. Plasticity of CD4+ FoxP3+ T cells. Curr. Opin. Immunol. **21:**281–285.